

RESEARCH LETTER

10.1002/2015GL064862

R. Marshall and C. da Silva contributed equally.

Key Points:

- Elve doublets are the ionospheric optical signature of compact intracloud discharges
- Elve doublets can be used to estimate the altitude and inclination angle of CIDs
- Many single elves may be mistakenly labeled as CG-generated when they are in fact CID-generated

Supporting Information:

- Movie S1
- Movie S1 caption

Correspondence to:

R. A. Marshall,  
ram80@stanford.edu

Citation:

Marshall, R. A., C. L. da Silva, and V. P. Pasko (2015), Elve doublets and compact intracloud discharges, *Geophys. Res. Lett.*, 42, 6112–6119, doi:10.1002/2015GL064862.

Received 8 JUN 2015

Accepted 1 JUL 2015

Accepted article online 4 JUL 2015

Published online 25 JUL 2015

Elve doublets and compact intracloud discharges

R. A. Marshall<sup>1,2</sup>, C. L. da Silva<sup>3</sup>, and V. P. Pasko<sup>3</sup>

<sup>1</sup>Department of Aeronautics and Astronautics, Stanford University, Stanford, California, USA, <sup>2</sup>Department of Aerospace Engineering Sciences, University of Colorado Boulder, Boulder, Colorado, USA, <sup>3</sup>Department of Electrical Engineering, Pennsylvania State University, University Park, Pennsylvania, USA

**Abstract** We present evidence of ionospheric optical signatures of lightning, known as elves, which sometimes occur in pairs separated in time by ~80–160 μs. We demonstrate that these “elve doublets” are the ionospheric signature of compact intracloud discharges (CIDs), which are extremely powerful, compact discharges that are thought to occur near the tops of thunderclouds. In this paper, using simple geometric calculations and full electromagnetic simulations, we show that CIDs from altitudes 14–22 km explain the time delay observed in elve doublets, consistent with typical CID altitudes. Furthermore, we show that the relative brightness of the first and second elves in the doublet is likely related to the orientation of the CID, and angles of 5°–20° with respect to the vertical are consistent with the observed brightness ratios.

1. Introduction

Compact intracloud discharges (CIDs), first reported by *Le Vine* [1980], are extremely powerful; compact discharges that are thought to occur near the tops of some thunderclouds. Over their short history of research they have also been referred to as narrow bipolar pulses or events (NBPs/NBEs) [*Smith et al.*, 1999; *Eack*, 2004], Narrow positive/negative bipolar pulses (NPBPs/NNBPs) [*Willett et al.*, 1989] and, when measured on orbit, transionospheric pulse pairs (TIPPs) [*Massey and Holden*, 1995; *Light and Jacobson*, 2002]. Using broadband fast electric field change (FEFC) measurements, *Willett et al.* [1989] showed that these events have durations of 20–30 μs. CIDs occur at unusually high altitudes, sometimes possibly above the tropopause in the overshooting tops of thunderclouds [*Nag et al.*, 2010], and have radiated field amplitudes similar to cloud-to-ground (CG) lightning and 10 times larger than typical intracloud (IC) lightning [*Smith et al.*, 1999].

The altitudes of CIDs are measured in two ways. For ground-based measurements, the time delay between two successive ionospheric reflections, together with the time delay of the ground wave, yields the altitude of the CID and the ionospheric reflection height [*Smith et al.*, 1999]. For space-based measurements, the altitude is given by the time delay between the direct signal and the ground-reflected signal. Using these methods, similar distributions of altitudes have been derived by different authors. *Smith et al.* [1999] found altitudes of 8–11 km using an array of FEFC meters and HF measurements; using the Los Alamos Sferic Array (LASA), *Smith et al.* [2004] found altitudes of 7–20 km, with a few as high as 30 km, for a distribution of over 100,000 events. Additionally, they found that positive-polarity events occurred below 15 km, while negative-polarity ones occurred above 15 km, likely between the upper positive charge layer and the negative screening charge layer at the top of the thundercloud. A summary on how the different-polarity CIDs are related to the thundercloud charge structure is provided by *da Silva and Pasko* [2015, Figure 3]. From FORTE satellite data, *Jacobson and Heavner* [2004] found that of over 20,000 CIDs, about 20% occurred above 15 km altitude. *Nag et al.* [2010] found altitudes from 6–30 km, with a mean of 16 km, for a data set of 48 CIDs.

CID amplitudes measured by *Nag et al.* [2010] showed normalized  $E_{100}$  amplitudes with a geometric mean of over 20 V/m, easily strong enough to cause electron-impact ionization in the lower ionosphere [e.g., *Taranenko et al.*, 1993]. Similarly, *Nag et al.* [2011] derived peak currents in CIDs from 33 to 259 kA, with a geometric mean of 74 kA, from the radiated fields; however, for CIDs the calibration from radiated fields to peak currents is not nearly as well established as it is for cloud-to-ground lightning. The true mechanism of CID source current is still under intense investigation. The observational fact that CIDs are very infrequently followed by radio signals of conventional intracloud lightning and the lack of substantial measurements of CIDs’ optical radiation has led a number of researchers in the past to suggest that CIDs are manifestations of relativistic runaway electron avalanches seeded by extensive air showers [see, e.g., *Dwyer and Uman*, 2014, section 6,

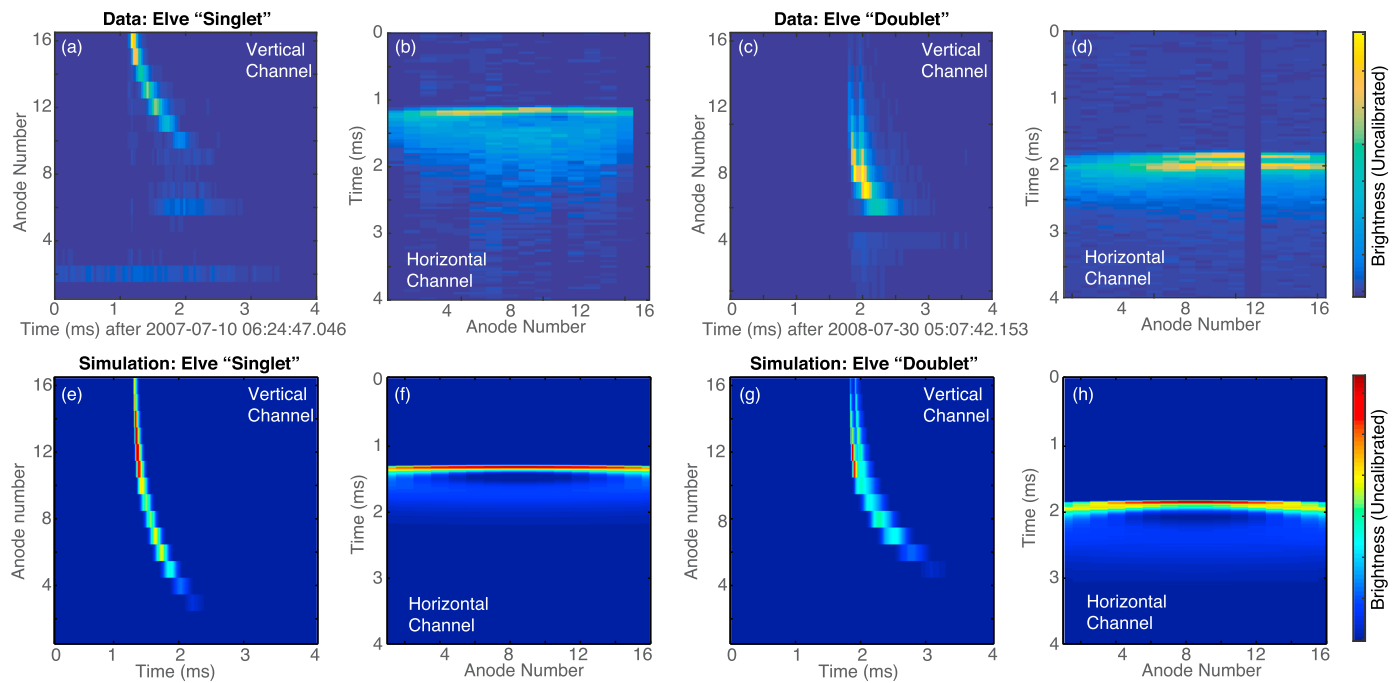


**Figure 1.** Example Elves, in (a–d) PIPER data and (e–h) EMP simulation. Figures 1a, 1b, 1e, and 1f show typical CG-generated elves, in the vertical and horizontal channels of PIPER, and a simulation to compare. Figures 1c, 1d, 1g, and 1h show an elve doublet with an identical arrangement. The doublet simulation was generated by a CID-like source at 20 km altitude. Note that the data and simulations do not have the same fields of view so do not match up perfectly.

and references therein]. More recently, *da Silva and Pasko* [2015] demonstrated that CIDs might be generated in an analogous process to initial breakdown pulses in intracloud lightning, showing in particular that a large step of an intracloud lightning leader can radiate broadband signals that are fully consistent with CID ground-based measurements. In their perspective, CIDs might be seen as an “attempted intracloud lightning discharge,” which after formation does not meet leader propagation criteria that allows further growth.

When the electromagnetic pulse (EMP) from an intense lightning return stroke reaches the lower ionosphere at ~85 km altitude (at night), it causes heating of the ionospheric electrons, produces new ionization, and produces optical emissions, known as “elves” [*Inan et al.*, 1991; *Fukunishi et al.*, 1996], which can be observed from the ground (using cameras and photometer arrays [*Fukunishi et al.*, 1996; *Newsome and Inan*, 2010]) or by using space-based instruments such as Imager of Sprites and Upper Atmospheric Lightning (ISUAL) [*Chern et al.*, 2003]. Results from ISUAL have shown that elves are the most common class of transient luminous events (TLEs) [*Chen et al.*, 2008].

Using the high-speed ground-based photometer array known as PIPER [*Marshall et al.*, 2008], *Newsome and Inan* [2010] observed over 1500 elves in the summers of 2007–2009 and found that a small fraction (~4%) of these are “elve doublets,” where two elves appear to occur with a very small time delay on the order of 100 μs. Examples of an elve and an elve doublet are shown in Figure 1. *Marshall* [2012] attributed these elve doublets to the double-peak of the current pulse with a risetime comparable to its fall time; however, the risetimes required in this scenario were unrealistic. The doublet-peak mechanism of *Marshall* [2012] requires risetimes of 40–70 μs; but measured risetimes for negative and positive cloud-to-ground discharges range from ~2–20 μs [e.g., *Berger et al.*, 1975] and ~3–25 μs, respectively [*Rakov and Uman*, 2003, Table 5.4]. However, we do not completely rule out this mechanism as a possible source of some elve doublets. *Newsome and Inan* [2010] further discussed a high-altitude source (18 km) and a ground reflection as a root cause of these events; however, further analysis was not undertaken at that time.

In this paper we show, using further analysis of the PIPER elve data along with new numerical simulations, that elve doublets are caused by CIDs. As such, this work shows that CIDs are powerful enough to create elves, which have a peak current threshold for production of 88 kA as noted above for CG lightning. We also demonstrate how elve doublets can be used to better understand CIDs, including their altitude, intensity, orientation, and other parameters.

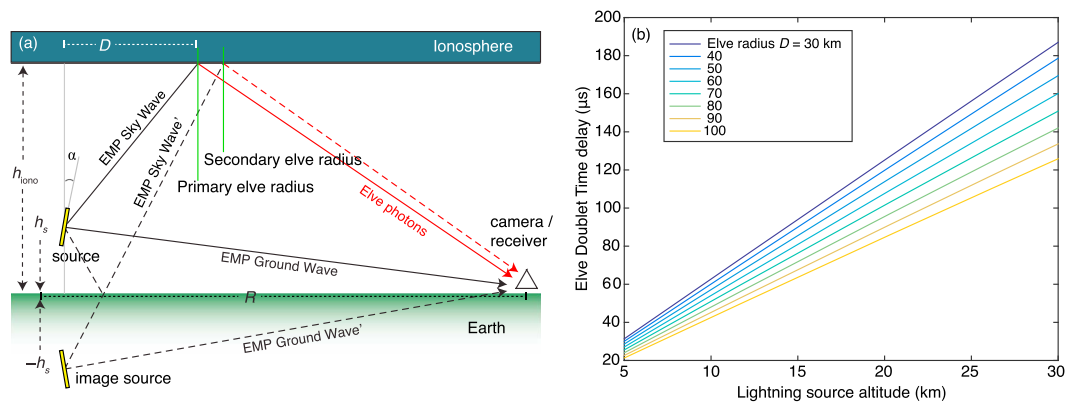


**Figure 2.** (a) Geometric interpretation of elve doublet generation from a CID source at altitude  $h_s$  with inclination  $\alpha$ . (b) Geometric calculations of the expected time delay versus altitude, for several elve radii, assuming that the source and its image produce elves with the same optical radii.

## 2. Elve Doublet Geometry

Figure 2a shows the source layout that leads to elve doublets. An IC discharge at an altitude  $h_s$  emits an EMP which radiates in all directions. The first elve in the doublet is created by the EMP direct path to the ionosphere; the second elve in the doublet is created by the ground reflection. The time difference between the two elve peaks depends on the altitude of the discharge, the altitude of the ionospheric reflection, and the distance to the camera, but the functional dependence on the source altitude  $h_s$  dominates. Note that the source in Figure 2a is oriented at an angle  $\alpha$  to the vertical; we discuss the implications of this angle in section 5.

Figure 2b shows an analytical estimate of elve doublet time delay assuming that both elves have the same optical radii  $D$  in the ionosphere (situated at height  $h_{iono} = 87$  km). The time delay is given by  $t_d = (d_2 - d_1)/c$ , where  $d_2$  and  $d_1$  are the distances from the source and the image source, respectively, to the ionosphere and are given by:

$$d_{2,1}^2 = (R_E \pm h_s)^2 + (R_E + h_{iono})^2 - 2(R_E \pm h_s)(R_E + h_{iono}) \cos(D/R_E) \quad (1)$$

where  $R_E$  is the radius of the Earth and all other parameters are given in the figure. The distances  $d_2$  and  $d_1$  are given by the “+” and “-” in the equation, respectively. Note that this calculation accounts for Earth curvature.

From this simple estimate we can see that source heights  $\gtrsim 18$  km are required to produce delays of  $\sim 120 \mu s$ , thus making negative-polarity CIDs, the highest-altitude intracloud lightning discharges ever observed (see e.g., *Smith et al.* [2004, Figure 5]), the likely source mechanism of the observed elve doublets. However, the observation of elve doublets is limited by the time resolution of the PIPER instrument; CIDs from lower altitudes may lead to elve doublets with shorter time delays than PIPER can resolve. We note that *Blaes et al.* [2014] found elve radii with a mean of 34 km; however, that radius is defined by the half maximum rather than the maximum and applies to elves presumably produced by cloud-to-ground lightning. The simulations described in section 4 show a typical radius of peak brightness for CIDs of  $\sim 75$  km.

## 3. Elve Doublet Data

For this report we utilize a data set of elves observed in the summers of 2007–2009. Over 1500 elves were observed using the PIPER photometer array, installed at Langmuir Laboratory (Socorro, NM) in 2008 and at Yucca Ridge Field Station (Fort Collins, CO) in 2007 and 2009. From the entire elve data set, 55 usable elve doublets were identified. *Newsome and Inan* [2010] reported on elve doublet “delays”—the delay time between the first and second elve in the doublet—with  $40 \mu s$  accuracy, consistent with the PIPER data resolution. In Figure 3a we reproduce the statistics of doublet delays; however, here we have interpolated the data with cubic splines to achieve resolution of  $20 \mu s$ . The delay time is calculated by finding the maximum delay among all PIPER channels. The histogram shown then reflects the average of the delays from the vertical and horizontal channels. We use the same approach when we estimate the simulated elve doublet delays in section 4.

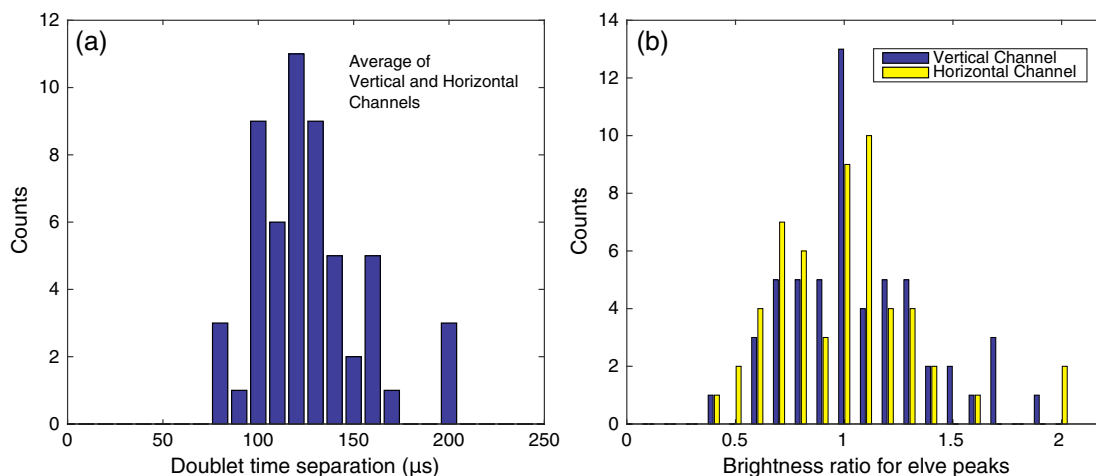


**Figure 3.** Elve doublet properties extracted from PIPER data taken in 2007–2009. (a) Extracted elve doublet delays. (b) Brightness ratios extracted from vertical and horizontal PIPER channels.

Figure 3b shows the ratio of the maximum brightness of the first elve to the second elve in each doublet; this is our convention for the brightness ratio throughout this paper. We observe that on average, the first and second elve have comparable peak brightness (ratio = 1). In many cases, the first elve of the doublet is brighter, with a peak ratio of up to 2; but in other cases, the second elve in the doublet can be the stronger of the two (ratio = 0.5). We will address these brightness ratios in section 5.

#### 4. Elve Doublet Simulations

We use the EMP model introduced by Marshall [2012] to simulate the lightning EMP and its interaction with the ground and ionosphere. The EMP model solves Maxwell's equations and the Langevin equation for a collisional magnetized plasma in a spherical coordinate system that naturally accounts for Earth curvature. It includes realistic ground, ionosphere, atmosphere, and geomagnetic field parameters and calculates electron heating, ionization, and optical emissions in the lower ionosphere. In these simulations we use a two-parameter Wait and Spies [1964] ionosphere model with  $h' = 87$  km (the reflection height) and  $\beta = 0.8$  (the ionosphere "sharpness"), consistent with values derived from measurements [e.g., Lay et al., 2014]. The azimuthally symmetric 2-D version of the EMP model is used for these simulations.

The CID source current is simulated with a modified transmission line model, where a current pulse with rise and fall described by Gaussian functions of time [e.g., Watson and Marshall, 2007] is injected at the top of a conducting channel with speed  $0.75 c$  in the downward direction. The current waveform rises from zero to peak in  $10 \mu s$  (with effective 10-to-90% risetime of  $3.2 \mu s$ ), and it decays to a  $1/e$  fraction of its peak value in  $15 \mu s$ . The transmission-line-model channel is 2 km long. The amplitude of current wave propagating in the channel is assumed to follow an asymmetric Gaussian distribution in the vertical direction. The source current peaks at height  $h_s$ , and it decreases to a fraction of  $10^{-3}$  of the peak value (i.e., approximately zero) at a distance of 1.4 and 0.6 km from  $h_s$ , below and above  $h_s$ , respectively, hence the asymmetry. Since we use Gaussian distributions to describe the source current variation in both space and time, we hereafter refer to this model as the Modified Transmission Line-Gaussian (MTLG) model. The adopted source current spatial distribution is analogous to the Modified Transmission Line-Kumaraswamy model used by Karunaratne et al. [2014, Figure 3b]. The generated source current with the proposed MTLG model is fully consistent with physics-based modeling of CID sources by da Silva and Pasko [2015]. Specifically, the fact that the current is zero in both channel extremities and peaks somewhere in the middle of it ensures charge neutrality at the source at all times. In the simulations presented in this paper, we only vary two parameters of the MTLG model: the peak current and source height ( $h_s$ ).

Along with observed PIPER elves, Figures 1e–1h show example of simulated elves as they would be measured by PIPER. For different CID altitudes and other parameter variations, we wish to estimate the elve doublet delay time and brightness ratio from these simulated PIPER images. We use the same methods as in the data to estimate both the delay and brightness ratio. Having assumed the CID altitudes from 8 to 26 km, and PIPER

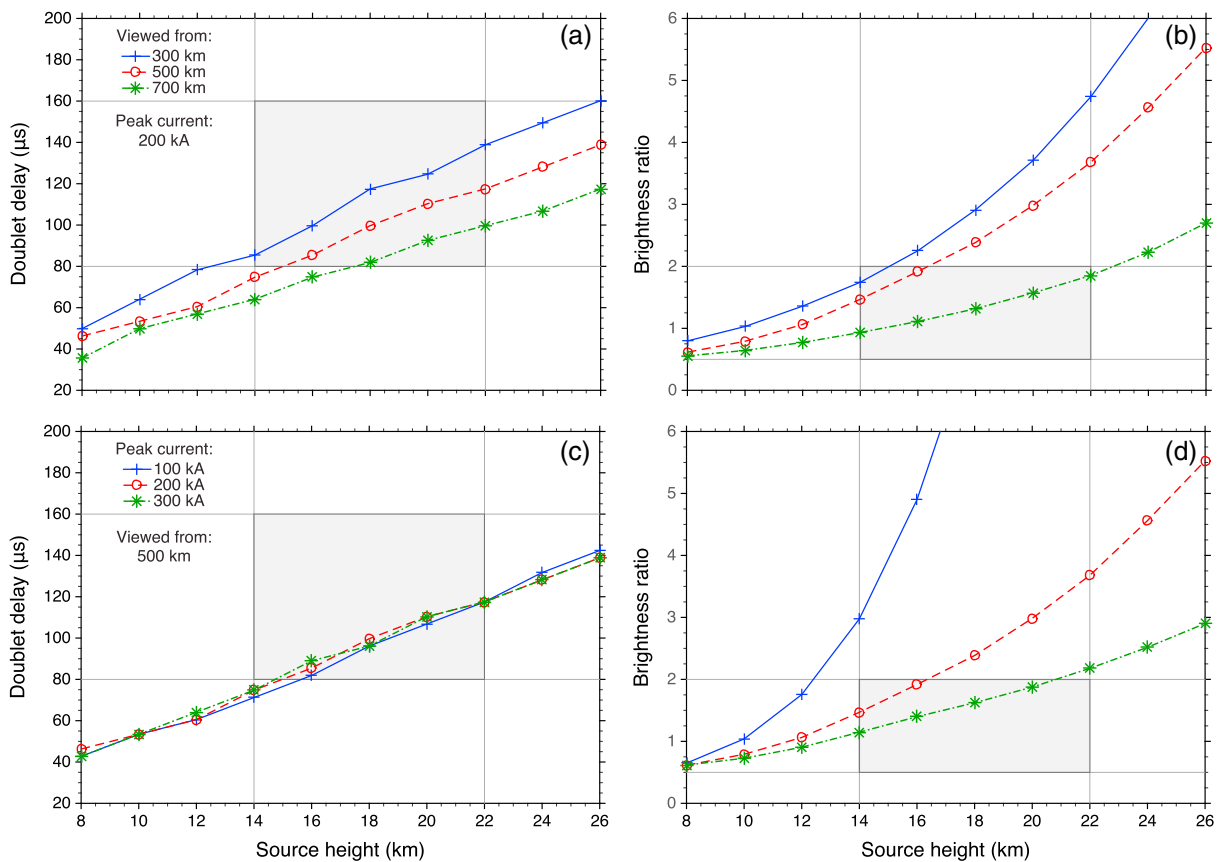


**Figure 4.** Simulation results using the MTLG model for the CID source current and the EMP model for electromagnetic field propagation and calculation of optical emissions. (a and b) The elve doublet time separation and (b and d) the brightness ratio versus CID altitude. Figures 4a and 4b show the effect of different viewing distances, while Figures 4c and 4d show the effect of source peak current. Note that PIPER elves have been observed at ranges from 250 km to 900 km. Brightness ratios are the ratio of the first elve to the second.

viewing locations from 300 to 700 km from the lightning source, Figure 4 shows the resulting time delays and brightness ratios. Figures 4a and 4b correspond to a 200 kA discharge, and the three curves represent different viewing distances. Figures 4c and 4d correspond to a viewing distance of 500 km, and the three curves represent different source peak currents. The gray box in each panel bounds the observed PIPER delays, from 80 to 160 μs, and the observed negative CID altitudes of 14–22 km, from *Smith et al.* [2004, Figure 5]. The simulated delays match both radio and optical observations very well and give evidence that these elve doublets are in fact the signatures of CIDs.

We observe from Figures 4a and 4c that the doublet delay increases approximately linearly with source altitude, as expected. Furthermore, from Figures 4b and 4d, the brightness ratio (ratio of first elve to second elve) increases nonlinearly with source altitude, due to the  $1/r$  fall off of the radiated electric field with distance. There is little to no effect on the time delay due to peak current (Figure 4c), as expected, but the brightness ratio is considerably higher for lower peak currents (Figure 4d). This effect arises due to the fact that the optical excitation rates saturate with very strong electric fields [e.g., *Liu and Pasko*, 2004, Figure 1c; *Marshall et al.*, 2010, Figure 3]; so while the electric field ratio in the ionosphere may be very high, the optical brightness ratio is lower.

We observe in Figure 4a that there is a significant variation in the delay time with distance between the source and observer. This variation can be explained with reference to Figure 2a: if the second elve in the doublet has a larger radius (verified by simulations), the time delay will be smaller because the second elve effectively happens closer to the observer. A scatterplot of elve doublet delays versus distance to the source (not included here for the sake of brevity) does not reflect this trend; however, that is not surprising because the altitudes are not known a priori.

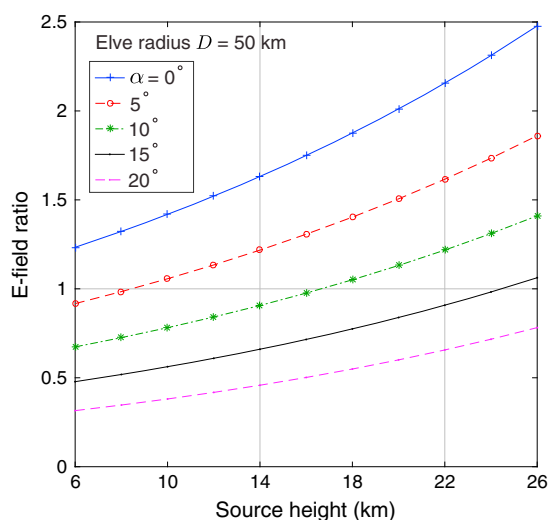


**Figure 5.** Analytical calculation of (elve-doublet-generating) electric field ratios for different CID source inclination angles from  $0^\circ$ – $20^\circ$ . The peak brightness of both elves in the doublet is assumed to occur at 50 km radius. Again, the ratio is defined as the peak of the first pulse divided by the peak of the second.

uniform distribution of source altitudes from 13 to 28 km. A few events are identified at 30 km or higher; however, that is likely due to the poor resolution of the PIPER data. A delay of only four samples corresponds to 160  $\mu$ s, and a few events were identified with five sample delays, or 200  $\mu$ s, leading to extremely high altitude estimates. PIPER-like measurements of elve doublets with higher time resolution are needed to more accurately estimate the source altitudes.

## 5. Doublet Brightness Ratios

The simulated brightness ratios of first elve to second elve in Figures 4b and 4d are always larger than one for source altitudes above 16 km, contrary to the histogram of measured brightness ratios in Figure 3 which are equally likely to be less than one. We modeled variation in the front speed of the downward-propagating current pulse and resulting radiation anisotropy [Tierney *et al.*, 2002], but simulation results demonstrate that the brightness ratio does not vary significantly. We believe that the inclination of the source current represents the most likely explanation.

The EMP model employed in the present study cannot simulate inclined sources. For this reason, we use an analytical approach, which assumes that the source behaves as an infinitesimal electrical dipole. The amplitude of the far-field vertical electric field at the surface of the conducting ionosphere, located at a height  $h_{\text{iono}}$ , generated by a small dipole located at height  $h_s$ , is proportional to  $\sin(\theta_1 - \alpha) / \sqrt{(h_{\text{iono}} - h_s)^2 + D^2}$ , where  $D$  is the elve hole radius and  $\theta_1 = \sin^{-1}(D / \sqrt{(h_{\text{iono}} - h_s)^2 + D^2})$ . A similar estimate can be made for the electric field from the ground image (see Figure 2a). Note that this calculation evaluates the elve-driving electric field at close radial distances and therefore is not sensitive to the effects of Earth curvature.

Figure 5 shows the ratio between the electric field produced by the (real) source current and its ground image, at a horizontal distance  $D = 50$  km from the source at an altitude  $h_{\text{iono}} = 90$  km. The figure shows the reference horizontal line  $E$  field ratio = 1, which corresponds to the data-inferred average brightness ratio = 1 in Figure 3b. Note that  $E$  field ratios above and below one are nonlinearly related to brightness ratios. The upward trend with altitude, which can also be seen in Figure 5, is precisely the effect that we hypothesized above as a source for the brightness ratios, but for the  $\alpha=0^\circ$  curve the ratio never falls below 1.2.

Nonetheless, these results show that a source inclined up to  $\alpha = 20^\circ$  can explain why the second elve in the doublet might be as bright as the first one (or even brighter in some cases). As such, we believe this is the most likely cause of the brightness ratios observed in Figure 3b. The inclination of source current has been previously suggested to be the mechanism responsible for explaining why the second VHF pulse in a TIPP can have higher energy than the first one [Massey and Holden, 1995].

From our data set of 55 usable elve doublets, only 20 had identifiable source currents as detected by National Lightning Detection Network (NLDN). The lack of NLDN matches lends further credence to the hypothesis that these are CIDs, because NLDN did not locate intracloud lightning with high efficiency in 2007–2009. This statement is supported by an experimental investigation made in 2005, prior to this period. Fleenor *et al.* [2009] used waveforms measured by LASA to check the NLDN classification of 417 cloud-to-ground (CG) lightning strokes. They concluded (see section 3.4.1 of their paper) that 33 (around 8%) of the classified NLDN CG strokes have LASA waveforms that are very similar to CIDs, except for the fact that they did not have a clear double ionospheric reflection (see Figure 10 of their paper).

Using Figure 4, with knowledge of the distance to the CID source (as located by the NLDN), we can interpolate to find the CID altitude. For the 20 events located by NLDN we find a relatively

It should be noted that model positive values  $\alpha \geq 0^\circ$ , as defined in Figure 2a, will always steer the peak of radiation toward the ground, leading to a lower brightness ratio; but real CIDs are just as likely to be inclined away from the observer. In those cases, the brightness ratio is likely so high that the second elve in the doublet is not observable, and the elve is interpreted to be a classic single CG-generated elve. As such, many of the 1500 elves observed by PIPER in 2007–2009, and identified as CG-generated elves, may in fact be also CID-generated elves.

## 6. Summary

We have shown that numerical simulations of compact intracloud discharges can reproduce the optical signatures of observed elve doublets and thus presented objective quantitative evidence that elve doublets are the ionospheric signatures of CIDs. These results further show that PIPER observations of elve doublets can be used to estimate the altitude of CID sources. We have shown that elve doublet brightness ratios—the ratio between the peak brightness of the first and second elves—can be explained by slightly inclined sources at angles up to  $20^\circ$ . These observations thus provide a new method to study CIDs.

It is worth noting that with  $40 \mu\text{s}$  resolution, PIPER may be limited to detecting CIDs at altitudes above  $\sim 10$ – $12$  km. CIDs may still occur at altitudes below 12 km but would be identified in PIPER data as single CG-generated elves, as the two parts of the elve will merge together. As mentioned earlier, higher time resolution data are necessary to identify elve doublets generated by lower altitude CIDs.

## Acknowledgments

This research was supported by NSF CEDAR grant AGS-1243176 to Stanford University and by NSF grant AGS-1332199 to Penn State University. The Stanford EMP model was developed under NSF grant AGS-1027070. The data and simulations used for this publication are available upon request from the authors.

The Editor thanks Abram Jacobson and an anonymous reviewer for their assistance evaluating this manuscript.

## References

- Berger, K., R. B. Anderson, and H. Kroninger (1975), Parameters of lightning flashes, *Electra*, *80*, 223–237.
- Blaes, P. R., R. A. Marshall, and U. S. Inan (2014), Return stroke speed of cloud-to-ground lightning estimated from elve hole radii, *Geophys. Res. Lett.*, *41*, 9182–9187, doi:10.1002/2014GL062392.
- Chen, A. B., et al. (2008), Global distributions and occurrence rates of transient luminous events, *J. Geophys. Res.*, *113*, A08306, doi:10.1029/2008JA013101.
- Chern, J. L., R. R. Hsu, H. T. Su, S. B. Mende, H. Fukunishi, Y. Takahashi, and L. C. Lee (2003), Global survey of upper atmospheric transient luminous events on the ROCSAT-2 satellite, *J. Atmos. Sol. Terr. Phys.*, *65*(5), 647–659.
- da Silva, C. L., and V. P. Pasko (2015), Physical mechanism of initial breakdown pulses and narrow bipolar events in lightning discharges, *J. Geophys. Res. Atmos.*, *120*, 4989–5009, doi:10.1002/2015JD023209.
- Dwyer, J. R., and M. A. Uman (2014), The physics of lightning, *Phys. Rep.*, *534*(4), 147–241, doi:10.1016/j.physrep.2013.09.004.
- Eack, K. B. (2004), Electrical characteristics of narrow bipolar events, *Geophys. Res. Lett.*, *31*, L20102, doi:10.1029/2004GL021117.
- Fleener, S. A., C. J. Biagi, K. L. Cummins, E. P. Krider, and X.-M. Shao (2009), Characteristics of cloud-to-ground lightning in warm-season thunderstorms in the Central Great Plains, *Atmos. Res.*, *91*(2), 333–352, doi:10.1016/j.atmosres.2008.08.011.
- Fukunishi, H., Y. Takahashi, M. Kubota, K. Sakanoi, U. S. Inan, and W. A. Lyons (1996), Elves: Lightning-induced transient luminous events in the lower ionosphere, *Geophys. Res. Lett.*, *23*, 2157–2160, doi:10.1029/96GL01979.
- Inan, U. S., T. F. Bell, and J. V. Rodriguez (1991), Heating and ionization of the lower ionosphere by lightning, *Geophys. Res. Lett.*, *18*(4), 705–708.
- Jacobson, A. R., and M. J. Heavner (2004), Comparison of narrow bipolar events with ordinary lightning as proxies for severe convection, *Mon. Weather Rev.*, *133*, 1144–1154.
- Karunaratne, S., T. C. Marshall, M. Stolzenburg, and N. Karunaratna (2014), Modeling initial breakdown pulses of CG lightning flashes, *J. Geophys. Res. Atmos.*, *119*, 9003–9019, doi:10.1002/2014JD021553.
- Lay, E. H., X.-M. Shao, and A. R. Jacobson (2014), D region electron profiles observed with substantial spatial and temporal change near thunderstorms, *J. Geophys. Res. Space Physics*, *119*, 4916–4928, doi:10.1002/2013JA019430.
- Le Vine, D. M. (1980), Sources of the strong rf radiation from lightning, *J. Geophys. Res.*, *85*(C7), 4091–4095.
- Light, T. E. L., and A. R. Jacobson (2002), Characteristics of impulsive VHF lightning signals observed by the FORTE satellite, *J. Geophys. Res.*, *107*(D24), 4756, doi:10.1029/2001JD001585.
- Liu, N. Y., and V. P. Pasko (2004), Effects of photoionization on propagation and branching of positive and negative streamers in sprites, *J. Geophys. Res.*, *109*, A04301, doi:10.1029/2003JA010064.
- Marshall, R. A. (2012), An improved model of the lightning electromagnetic field interaction with the D-region ionosphere, *J. Geophys. Res.*, *117*, A03316, doi:10.1029/2011JA017408.
- Marshall, R. A., R. T. Newsome, and U. S. Inan (2008), Fast photometric imaging using orthogonal linear arrays, *IEEE Trans. Geosci. Remote Sens.*, *46*(11), 3885–3893.
- Marshall, R. A., U. S. Inan, and V. S. Glukhov (2010), Elves and associated electron density changes due to cloud-to-ground and in-cloud lightning discharges, *J. Geophys. Res.*, *115*, A00E17, doi:10.1029/2009JA014469.
- Massey, R. S., and D. N. Holden (1995), Phenomenology of trans-ionospheric pulse pairs, *Radio Sci.*, *30*, 1645–1659.
- Nag, A., V. A. Rakov, D. Tsalikis, and J. A. Cramer (2010), On phenomenology of compact intracloud lightning discharges, *J. Geophys. Res.*, *115*, D14115, doi:10.1029/2009JD012957.
- Nag, A., V. A. Rakov, and J. A. Cramer (2011), Remote measurements of currents in cloud lightning discharges, *IEEE Trans. Electromagn. Compat.*, *53*(2), 407–413.
- Newsome, R. T., and U. S. Inan (2010), Free-running ground-based photometric array imaging of transient luminous events, *J. Geophys. Res.*, *115*, A00E41, doi:10.1029/2009JA014834.
- Rakov, V. A., and M. A. Uman (2003), *Lightning: Physics and Effects*, Cambridge Univ. Press, Cambridge, U. K.
- Smith, D. A., X. M. Shao, D. N. Holden, C. T. Rhodes, M. Brook, P. R. Krehbiel, M. Stanley, W. Rison, and R. J. Thomas (1999), A distinct class of isolated intracloud lightning discharges and their associated radio emissions, *J. Geophys. Res.*, *104*, 4189–4212.

- Smith, D. A., M. J. Heavner, A. R. Jacobson, X. M. Shao, R. S. Massey, R. J. Sheldon, and K. C. Wiens (2004), A method for determining intracloud lightning and ionospheric heights from VLF/LF electric field records, *Radio Sci.*, *39*, RS1010, doi:10.1029/2002RS002790.
- Taranenko, Y. N., U. S. Inan, and T. F. Bell (1993), The interaction with the lower ionosphere of electromagnetic pulses from lightning: Heating, attachment, and ionization, *Geophys. Res. Lett.*, *20*(15), 1539–1542.
- Tierney, H. E., A. R. Jacobson, R. Roussel-Dupre, and W. H. Beasley (2002), Transionospheric pulse pairs originating in maritime, continental, and coastal thunderstorms: Pulse energy ratios, *Radio Sci.*, *37*(3), 11-1–11-7, doi:10.1029/2001RS002506.
- Wait, J. R., and K. P. Spies (1964), Characteristics of the Earth-ionosphere waveguide for VLF radio waves, *Tech. Note 300*, Natl. Bur. of Stand., Boulder, Colo.
- Watson, S. S., and T. C. Marshall (2007), Current propagation model for a narrow bipolar pulse, *Geophys. Res. Lett.*, *34*, L04816, doi:10.1029/2006GL027426.
- Willett, J. C., J. C. Bailey, and E. P. Krider (1989), A class of unusual lightning electric field waveforms with very strong high-frequency radiation, *J. Geophys. Res.*, *94*(D13), 16,255–16,267.